

Sensitivity of Crossflow to Parametric Study of Complete Pressure Distribution Model for Horizontal Well in a Two-Layered Bounded Extended Reservoir

Ogbue M.C.

Department of Petroleum Engineering,
Delta State University, Abraka, Oleh Campus, P. M. B. 22, Oleh, Delta State, Nigeria.

Corresponding author: mogbue@delsu.edu.ng

Abstract

A crossflow interface acts as a constant pressure external boundary. It provides recharge of energy within a layer by fluid influx from another layer. The extent of recharge is determined by the degree of crossflow. Since there is no direct way to determine the degree of crossflow at the scale of a reservoir, parameters that control the behavior of crossflow were used to study its effect on pressure responses. This article is aimed at determining the sensitivity of crossflow to changes in the values of the parameters that control its performance in a two-layered bounded reservoir. Conceptual, physical, and mathematical models were sequentially developed for a horizontal well in a two-layered bounded reservoir with a crossflow interface. A mathematical model for the crossflow interface was derived as a function of fluid properties, reservoir properties, and real time. Quantifying parameters were defined as degree of crossflow, D , and ease of crossflow, E . Various configurations of the two-layered reservoir, resulting in eighteen sets of data, were used to study behaviour of Crossflow. From the results obtained, the degree of crossflow increases as the dimensionless pressure reduces. As ease of crossflow increases, so also does the rate of decline in pressure derivative. Degree of crossflow varies directly as dimensionless well standoff, dimensionless well radius, and dimensionless well length. The degree of crossflow varies inversely as the time normalization factor, dimensionless reservoir width, and dimensionless reservoir length. However, the degree of crossflow is not affected by reservoir thickness and interlayer mobility ratio. Ease of crossflow varies directly as interlayer mobility ratio, dimensionless well length, and dimensionless well radius but inversely as dimensionless well standoff, dimensionless reservoir length, and dimensionless reservoir width. But ease of crossflow is not affected by reservoir thickness. It was observed that optimum oil production and effective reservoir management can be achieved if both layers are produced from the layer with higher mobility. It is therefore recommendable as the best completion strategy for a layered reservoir with a crossflow interface to produce both layers from the layer with higher mobility.

Keywords: *Two-layered reservoir, horizontal well, crossflow, parametric study, unlimited number of flow regimes, pressure distribution model.*

1.0 Introduction

A crossflow interface allows the flow of fluid from one layer to another. Pressure distribution of a layered reservoir is affected by many factors. Studies have shown that transient pressure of a horizontal well in a layered reservoir is controlled by the degree of crossflow at the interface (Bourdet, 1985). It was reported that the seepage capacity of the interface between layers is a controlling factor in the pressure response of a horizontal well in a layered reservoir. Studies have shown that when crossflow stabilizes, the permeability with

which fluid flows is the result of the combined permeabilities of the two layers contributing to flow (Russel *et al.* 1962).

Studies have shown that in a dual-porosity system, when a horizontal well is used to produce from a higher permeability layer, two linear flows will occur: linear horizontal in the more permeable zone and linear vertical in the tight zone. The bilinear flow period is attributable to average effects of the two layers (Bourdet, 1985; Du *et al.* 1992). Changes in gradient in the log-log plot of dimensionless pressure versus dimensionless time, especially at late time, have been attributed to the effect of layering. The different gradients indicate the various contributions to flow, which are proportional to local permeabilities of those layers (Owolabi *et al.* 2012). In layered reservoirs, pressure responses have been observed to be functions of reservoir system parameters (Adewole *et al.*, 2003). Studies on crossflow interface in multilayer reservoirs (Kuchuk *et al.* 1996; Lu *et al.* 2021) have revealed distinctive behaviour in horizontal well performance.

Results have shown that each layer produces independently in a multi-layer system (Lu *et al.* 2021). A new analytical solution to determine individual layer properties in a multi-layer reservoir has been derived (Ehlig-Economides *et al.* 1995). An article on the performance of horizontal wells in layered reservoirs with simultaneous gas cap and bottom water drives has shown that a constant boundary effect on pressure distribution results at the late time flow period (Oloro *et al.* 2012). The study of crossflow was extended to multilayered radially composite reservoirs, and an analytical model for pressure behavior was developed. The characteristic constant pressure behavior during the boundary-dominated flow period was identified in article (Viana *et al.* 2022). Through the use of semi-analytical model rate decline curves for multiple-fractured horizontal wells in heterogeneous reservoirs, source function with boundary element method was studied (Wang *et al.*, 2017). Literature usually considers six of five flow regimes as the possible flow regimes in reservoirs produced by horizontal wells (Odeh *et al.* 1990; Kuchuk *et al.* 1996; Du *et al.* 1992; Al Rbeawi *et al.* 2013). By change in conceptual model, two new flow regimes peculiar to multiple horizontal fractures were shown to exist, in contrast to a single horizontal fracture (Chu *et al.*, 2019).

Recent research works have shown new additional flow regimes that hitherto were not considered in the pressure distribution of horizontal wells in layered reservoirs. The existing model largely restricted the number of flow regimes possible for a horizontal well in a reservoir through simplifying assumptions and a conceptual model. In such cases, flow regimes were considered to be determined by the geometry of the reservoir only. A review of existing literature suggests that flow regimes of horizontal wells in layered reservoirs are determined by fluid properties, rock properties, and the geometry of the reservoir. Approached in this context, more possible flow regimes of the reservoir system can be discovered. Therefore, in this paper, the responsiveness of the crossflow interface to the parametric study of pressure distribution was investigated. The possible flow regimes of a horizontal well in a two-layered bounded reservoir were also considered.

2. 0 Materials and Method

A conceptual model is developed from which a physical model and subsequent mathematical model were derived. Flow regimes were delineated. Input data was processed. Pressure distribution was generated from a mathematical model followed by analyses of pressure distribution.

2.1 Conceptual Model

Consider a reservoir consisting of two layers of different petrophysical properties. The layers are separated by a permeable interface, hence regarded as a crossflow interface. The interface is characterized by its degree of crossflow, which defines its capacity to allow fluid to crossflow from one layer to another. Another characteristic feature of a crossflow interface is its Ease, E , of crossflow, which defines its ease with which it allows seepage of fluid from one layer to the other. Crossflow causes changes in the pressure response of the well. The effect of interface on pressure is represented by individual layer factors A and B .

2.2 Physical Model

The Physical Model is presented in Figure 1 as a 3D reservoir.

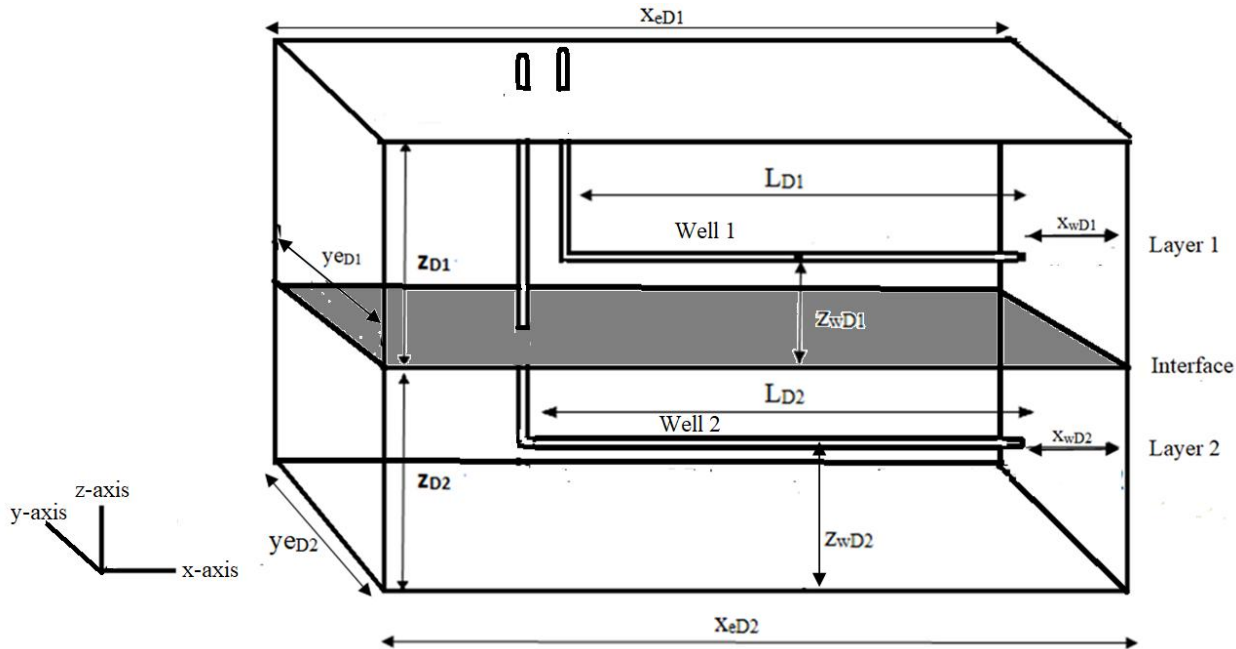


Figure 1: Physical model presented as 3D Layered Reservoir.

Three principal axes of flow, designated as the x-axis, y-axis, and z-axis, have been adopted. These axes represent the three principal axes of permeability, where, and represent permeability along the x-axis, y-axis and z-axis respectively. The anisotropy of the reservoir is defined such that, Heterogeneity of the reservoir is defined as, where and are porosity values of layer 1 and layer 2 respectively. Also, heterogeneity of the reservoir is defined as, where and are total compressibility values of layer 1 and layer 2 respectively. The following assumptions were made:

- (1) The reservoir has uniform thickness, it is horizontal, and external boundaries are closed.
- (2) Properties within a layer are uniform but differ from properties outside the layer.
- (3) Fluid flows from the reservoir to the well at a constant rate and as a single phase.
- (4) Interface spreads across the entire length of the reservoir.
- (5) Properties of the interface are uniform along its whole length.

2.3 Mathematical Model

Mathematical model is in form of dimensionless pressure, P_D , and dimensionless pressure derivative, P'_D functions of reservoir system parameters and fluid properties. Mathematical model was derived employing instantaneous Source term and Green's function proposed for constant-rate model (Gringarten *et al.* 1973). The mathematical expression is written down Newman product rule as:

Layer 1

Dimensionless Pressure is as shown in Equation (1)

$$\begin{aligned}
 P_{D1} = & 2\pi h_{D1} \int_0^{t_{D1}} ii(x).i(y).i(z)d\tau \\
 & + 2\pi h_{D1} \int_{t_{D2}}^{t_{D3}} ii(x).i(y).i(z)d\tau \\
 & + 2\pi h_{D1} A \int_{t_{D5}}^{t_{D2}} ii(x).i(y).ix(z)'d\tau \\
 & + 2\pi h_{D1} \int_{t_{D6}}^{t_{D4}} ii(x).vii(y).i(z)d\tau + 2\pi h_{D1} A \int_{t_{D8}}^{t_{D9}} ii(x).i(y).ix(z)'d\tau \\
 & + 2\pi h_{D1} \int_{t_{D10}}^{t_{D7}} ii(x).vii(y).i(z)d\tau \\
 & + 2\pi h_{D1} \int_{t_{D11}}^{t_{D8}} x(x).i(y).i(z)d\tau + 2\pi h_{D1} A \int_{t_{D12}}^{t_{D13}} x(x).i(y).ix(z)'d\tau \\
 & + 2\pi h_{D1} \int_{t_{D3}}^{t_{D8}} ii(x).i(y).i(z)d\tau + 2\pi h_{D1} \int_{t_{D14}}^{t_{D15}} x(x).vii(y).i(z)d\tau \\
 & + 2\pi h_{D1} A \int_{t_{D16}}^{t_{D2}} ii(x).vii(y).ix(z)'d\tau + 2\pi h_{D1} A \int_{t_{D18}}^{t_{D19}} x(x).vii(y).ix(z)'d\tau \quad (1)
 \end{aligned}$$

And the dimensionless pressure derivative is as shown in Equation (2) as

$$\begin{aligned}
 P'_{D1} = & 2\pi h_{D1} [ii(x).i(y).i(z)] + 2\pi h_{D1} [ii(x).i(y).i(z)] + 2\pi h_{D1} A [ii(x).i(y).ix(z)'] \\
 & + 2\pi h_{D1} [ii(x).vii(y).i(z)] + 2\pi h_{D1} A [ii(x).i(y).ix(z)'] + 2\pi h_{D1} [ii(x).vii(y).i(z)] \\
 & + 2\pi h_{D1} [x(x).i(y).i(z)] + 2\pi h_{D1} A [x(x).i(y).ix(z)'] + 2\pi h_{D1} [ii(x).i(y).i(z)] \\
 & + 2\pi h_{D1} [x(x).vii(y).i(z)] + 2\pi h_{D1} A [ii(x).vii(y).ix(z)'] \\
 & + 2\pi h_{D1} A [x(x).vii(y).ix(z)'] \quad (2)
 \end{aligned}$$

Constant, A, is only applicable to flow regimes that have felt the interface as one of its boundaries. Therefore, if the interface is not felt the constant, A, is not included in the integrand representing the flow regime.

Layer 2

The dimensionless pressure for Layer 2 is as written in Equation (3)

$$\begin{aligned}
 P_{D2} = & 2\pi h_{D2} \int_0^{\alpha t_{D1}} ii(x).i(y).i(z)d\tau \\
 & + 2\pi h_{D2} \int_{\alpha t_{D2}}^{\alpha t_{D3}} ii(x).i(y).i(z)d\tau \\
 & + 2\pi h_{D2} B \int_{\alpha t_{D4}}^{\alpha t_{D5}} ii(x).i(y).ix(z)d\tau \\
 & + 2\pi h_{D2} \int_{\alpha t_{D6}}^{\alpha t_{D7}} ii(x).vii(y).i(z)d\tau + 2\pi h_{D2} B \int_{\alpha t_{D8}}^{\alpha t_{D9}} ii(x).i(y).ix(z)d\tau \\
 & + 2\pi h_{D2} \int_{\alpha t_{D10}}^{\alpha t_{D11}} ii(x).vii(y).i(z)d\tau \\
 & + 2\pi h_{D2} \int_{\alpha t_{D12}}^{\alpha t_{D13}} x(x).i(y).i(z)d\tau + 2\pi h_{D2} B \int_{\alpha t_{D14}}^{\alpha t_{D15}} x(x).i(y).ix(z)d\tau \\
 & + 2\pi h_{D2} \int_{\alpha t_{D16}}^{\alpha t_{D17}} ii(x).i(y).i(z)d\tau + 2\pi h_{D2} \int_{\alpha t_{D18}}^{\alpha t_{D19}} x(x).vii(y).i(z)d\tau \\
 & + 2\pi h_{D2} B \int_{\alpha t_{D20}}^{\alpha t_{D21}} ii(x).vii(y).ix(z)d\tau \\
 & + 2\pi h_{D2} B \int_{\alpha t_{D22}}^{\alpha t_{D23}} x(x).vii(y).ix(z)d\tau
 \end{aligned} \tag{3}$$

The dimensionless pressure derivative is as shown in Equation (4);

$$\begin{aligned}
 P'_{D2} = & 2\pi h_{D2} [ii(x).i(y).i(z)] + 2\pi h_{D2} [ii(x).i(y).i(z)] + 2\pi h_{D2} B [ii(x).i(y).ix(z)] + 2\pi h_{D2} [ii(x).vii(y).i(z)] \\
 & + 2\pi h_{D2} B [ii(x).i(y).ix(z)] + 2\pi h_{D2} [ii(x).vii(y).i(z)] + 2\pi h_{D2} [x(x).i(y).i(z)] + 2\pi h_{D2} B [x(x).i(y).ix(z)] \\
 & + 2\pi h_{D2} [ii(x).i(y).i(z)] + 2\pi h_{D2} [x(x).vii(y).i(z)] + 2\pi h_{D2} B [ii(x).vii(y).ix(z)] \\
 & + 2\pi h_{D2} B [x(x).vii(y).ix(z)]
 \end{aligned} \tag{4}$$

Constant, B, is only applicable to flow regimes that have felt the interface as one of its boundaries.

Individual layer modification factors, A and B, modify source functions to layered reservoir along the z-axes for crossflow interface. Each weighs effect of crossflow along z-axis on pressure response (Owolabi *et al.*, 2012). By applying some boundary conditions at the interface, factors were derived:

Pressure in Layer 1 equals pressure in layer 2, was expressed in dimensional form as Equation (5).

$$P_{D1} = P_{D2} \tag{5}$$

Velocity of fluid in Layer 1 equals velocity in Layer 2, which could be expressed in dimensionless form (Equation (6)).

$$\frac{\partial P_{D1}}{\partial z_D} = M \frac{\partial P_{D2}}{\partial z_D} \quad (6) \quad \text{Where } M \text{ is}$$

interlayer mobility ratio given in Equation (7) as:

$$M = \frac{K_2 \mu_1}{K_1 \mu_2} \quad (7)$$

Where K_1 and K_2 are permeability values in layer 1 and 2 respectively, μ_1 and μ_2 are viscosity values in layer 1 and 2 respectively, α is time normalization factor of Layer 2 responses with respect to Layer 1 given as Equation (8).

$$\alpha = \frac{\phi_1 \mu_1 C_{t1} L_1^2 K_2 t_2}{\phi_2 \mu_2 C_{t2} L_2^2 K_1 t_1} \quad (8)$$

2.4. Description of Variables used for Quantifying Crossflow

For easy analysis of crossflow, some variables have been introduced in the log-log plot of dimensionless pressure and dimensionless pressure derivative as shown in Figure 2.

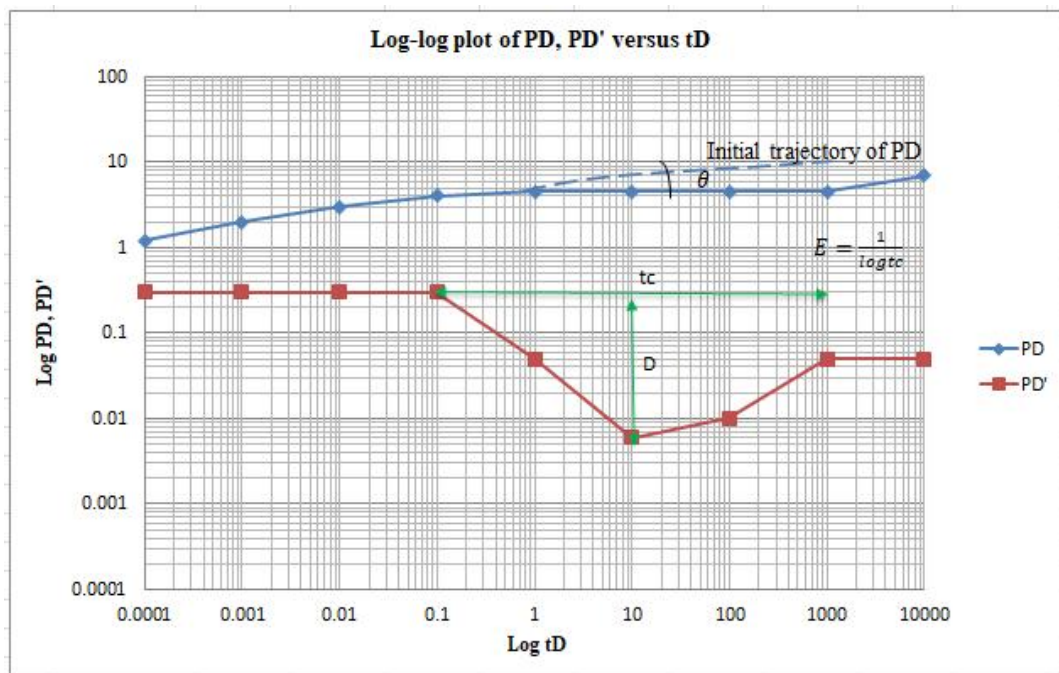


Figure 2: Quantitative characterization of crossflow using variables: Degree of crossflow, D (θ), and Ease of crossflow, E .

In the pressure distribution plots, as shown in Figure 2, the Ease of crossflow, E , is described as the reciprocal of log time interval, t_c , between when the effect of crossflow commenced and when it is fully established. It measures how rapid crossflow is fully established. High value of E implies that there is easy crossflow through the interface. Degree of crossflow, D , is described as the extent of crossflow between layers. It is quantified as extent of decline of dimensionless pressure derivative as crossflow is felt. It bears strong relationship with angle of deviation, θ . Angle of deviation, θ , is quantified as angle of deviation from the initial trajectory of dimensionless pressure as crossflow is felt. For high values of degree of crossflow, D , there is active influx of fluid, thus the interface behaves like constant pressure boundary. Similarly, θ will be high.

3.0 Results and Discussion

3.1 Model Validation

The Viana *et al.* (2022) model was used to validate the model of this article. The data used are shown in Table 2. In this stage, the effect of crossflow contained in this model was verified by comparing it with effect of crossflow contained in established model. In this analysis, it was assumed that only Layer 1 was completed and produced from, while crossflow from Layer 2 was amenable. The pressure distribution of Layer 1 is as shown in Figure 3. During formation crossflow, fluid flow from Layer 2 to Layer 1. Curves of P_D values obtained from model of this article was observed to be higher than those obtained from Viana *et al.* However, close match was observed between the two models. Due to presence of crossflow after $t_D=1$, P_D was shown to tend towards a constant value with time, while P_D' was shown to slope downwards with time. The effect of crossflow was manifested as a steady state behavior as shown also by Viana *et al.* (Viana *et al.*, 2022).

Table 2: Reservoir System Parameters used for Validation of Model using Viana *et al* model.

Case	Properties	Layer1,	Layer2,
D2	r(m)	15	15
	K (md)	500	3000
	h(m)	15	25
	μ (cp)	5.1	10.2

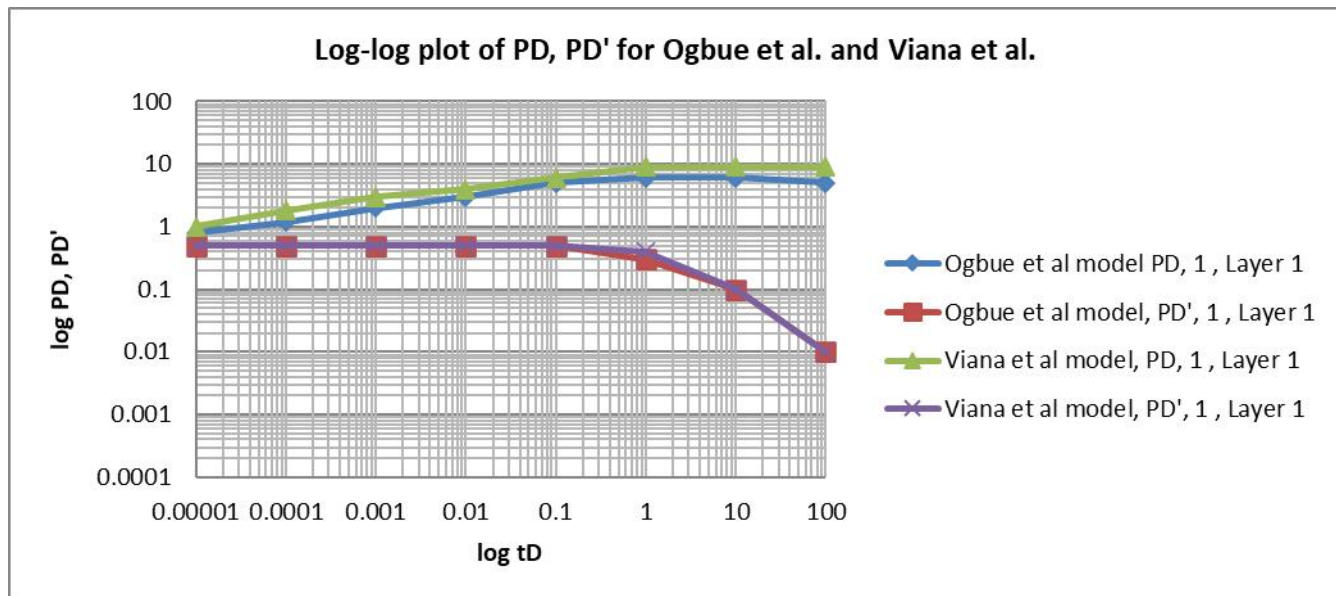


Figure 3: Comparison with the results from Ogbue's model and Viana's model for crossflow and no crossflow on log-log plot.

3.2 Responsiveness of Crossflow to Parametric Study of Complete Pressure Distribution Model

Seventeen cases of reservoir system parameters were considered as shown in Table 3. These parameters were given in dimensionless form as defined in the Appendix, Equations (9) to (24).

Case 1 was used as the basis from which variation of values of parameters were made. Thus, it was the basis of comparison to determine the effect of change in values of parameters. As pressure transient got to a crossflow interface, there was flattening of dimensionless pressure and decline in dimensionless pressure derivative. After a time, the trend would stop when the crossflow has been fully established. Then pressure response of each layer stabilizes to become the same (Bourdet, 1985; Adewole *et al.*, 2003). Afterwards, flow becomes the

combined effect of the two layers. From the pressure distribution plots, the Ease of crossflow, E , was measured. Degree of crossflow was also measured.

Table 3: Sampling of Data for Sensitivity Analyses of Pressure Distribution of Model with Reservoir System Parameter.

Sample	Layer	x_{eD}	x_{wD}	D_{xD}	y_{wD}	y_{eD}	z_{wD}	Z_{eD}	L_D	r_{wD}	α	M
1	1	5.0	2.5	1.25	2.5	5.0	0.024	0.05	2.5	0.001	5.0	1.0
	2	5.0	2.5	1.25	2.5	5.0	0.024	0.05	2.5	0.001	5.0	1.0
2	1	5.0	2.5	1.25	2.5	5.0	0.009	0.02	2.5	0.001	5.0	1.0
	2	5.0	2.5	1.25	2.5	5.0	0.009	0.02	2.5	0.001	5.0	1.0
3	1	5.0	2.5	1.25	2.5	5.0	0.004	0.01	2.5	0.001	5.0	1.0
	2	5.0	2.5	1.25	2.5	5.0	0.004	0.01	2.5	0.001	5.0	1.0
4	1	5.0	2.5	1.25	2.5	5.0	0.049	0.10	2.5	0.001	5.0	1.0
	2	5.0	2.5	1.25	2.5	5.0	0.049	0.10	2.5	0.001	5.0	1.0
5	1	5.0	2.5	1.25	2.5	5.0	0.999	0.20	2.5	0.001	5.0	1.0
	2	5.0	2.5	1.25	2.5	5.0	0.999	0.20	2.5	0.001	5.0	1.0
6	1	5.0	2.5	1.25	2.5	5.0	0.015	0.05	2.5	0.01	5.0	1.0
	2	5.0	2.5	1.25	2.5	5.0	0.015	0.05	2.5	0.01	5.0	1.0
7	1	5.0	2.5	1.25	2.5	5.0	0.0249	0.05	2.5	0.0001	5.0	1.0
	2	5.0	2.5	1.25	2.5	5.0	0.0249	0.05	2.5	0.0001	5.0	1.0
8	1	5.0	2.5	0.50	2.5	5.0	0.024	0.05	4.0	0.001	5.0	1.0
	2	5.0	2.5	0.50	2.5	5.0	0.024	0.05	4.0	0.001	5.0	1.0
9	1	5.0	2.5	2.00	2.5	5.0	0.024	0.05	1.0	0.001	5.0	1.0
	2	5.0	2.5	2.00	2.5	5.0	0.024	0.05	1.0	0.001	5.0	1.0
10	1	3.0	1.5	0.25	2.5	5.0	0.024	0.05	2.5	0.001	5.0	1.0
	2	3.0	1.5	0.25	2.5	5.0	0.024	0.05	2.5	0.001	5.0	1.0
11	1	7.5	3.75	2.50	2.5	5.0	0.024	0.05	2.5	0.001	5.0	1.0
	2	7.5	3.75	2.50	2.5	5.0	0.024	0.05	2.5	0.001	5.0	1.0
12	1	5.0	2.5	1.25	1.5	3.0	0.024	0.05	2.5	0.001	5.0	1.0
	2	5.0	2.5	1.25	1.5	3.0	0.024	0.05	2.5	0.001	5.0	1.0
13	1	5.0	2.5	1.25	3.5	7.0	0.024	0.05	2.5	0.001	5.0	1.0
	2	5.0	2.5	1.25	3.5	7.0	0.024	0.05	2.5	0.001	5.0	1.0
14	1	5.0	2.5	1.25	2.5	5.0	0.024	0.05	2.5	0.001	0.5	1.0
	2	5.0	2.5	1.25	2.5	5.0	0.024	0.05	2.5	0.001	0.5	1.0
15	1	5.0	2.5	1.25	2.5	5.0	0.024	0.05	2.5	0.001	1.0	1.0
	2	5.0	2.5	1.25	2.5	5.0	0.024	0.05	2.5	0.001	1.0	1.0
16	1	5.0	2.5	1.25	2.5	5.0	0.024	0.05	2.5	0.001	5.0	0.5
	2	5.0	2.5	1.25	2.5	5.0	0.024	0.05	2.5	0.001	5.0	0.5
17	1	5.0	2.5	1.25	2.5	5.0	0.024	0.05	2.5	0.001	5.0	5.0
	2	5.0	2.5	1.25	2.5	5.0	0.024	0.05	2.5	0.001	5.0	5.0

3.2.1. Effect of dimensionless reservoir thickness, z_{eD} and dimensionless well standoff, z_{wD} on crossflow

Cases 2 to 5 were variation of dimensionless reservoir thickness, z_{eD} and dimensionless well standoff, z_{wD} . Thus, effect of variation of reservoir thickness and well standoff was studied and shown in Figure 4. As shown in Figure 4, as reservoir thickness increases, the rate of decline in pressure increases. Dimensionless pressure increases as reservoir thickness increases. As shown also, as dimensionless standoff increases, ease of crossflow reduces. Degree of crossflow was observed to be similar.

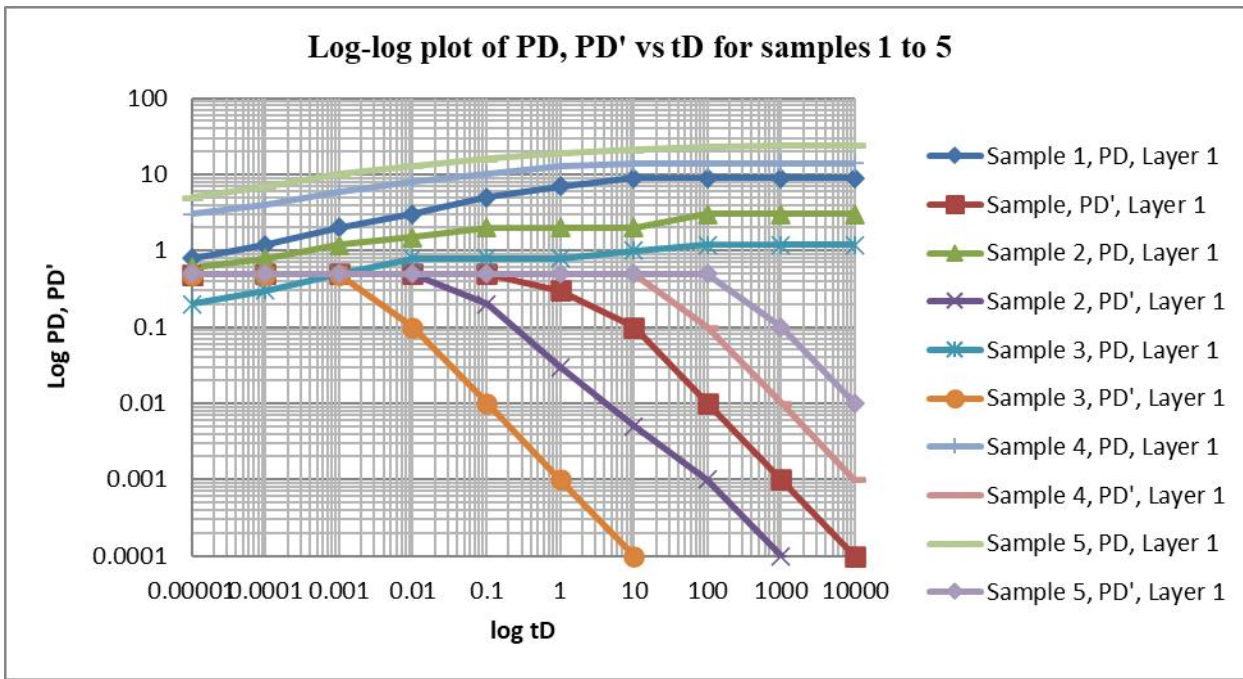


Figure 4: Assessment of response of crossflow due to effect variation of dimensionless reservoir thickness, z_{eD} and dimensionless well standoff, z_{wD} .

3.2.2. Effect of dimensionless well radius, r_{wD} on crossflow

Cases 6 and 7 were variation of dimensionless well radius, r_{wD} . Thus, effect of variation of well radius was studied as shown in Figure 5. As shown in Figure 5, as well radius increases, the rate of decline in pressure increases. Dimensionless pressure increases as well radius increases. As dimensionless well radius increases, there is ease of crossflow and degree of crossflow.

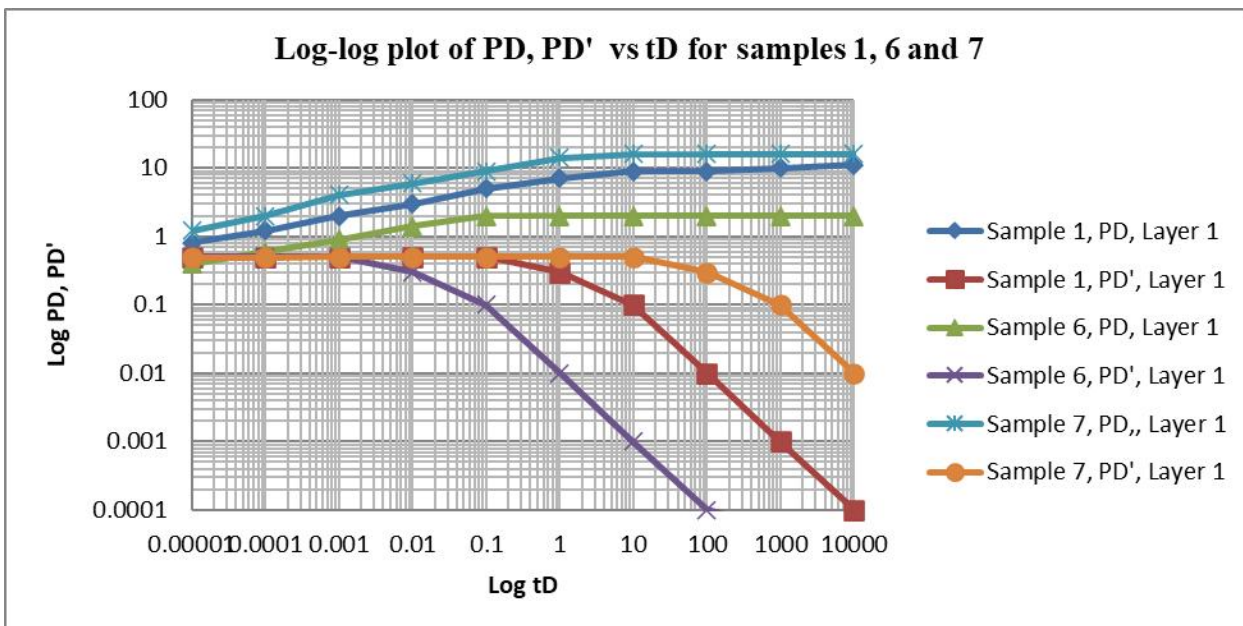


Figure 5: Assessment of response of crossflow due to effect variation of dimensionless well radius, r_{wD} .

3.2.3. Effect of dimensionless well length, L_D and dimensionless distance from tip of well to the lateral boundary of the reservoir, D_{xD} on crossflow

Cases 8 and 9 were variation of dimensionless well length, L_D and dimensionless distance from tip of well to the lateral boundary of the reservoir, D_{xD} . Thus, as shown in Figure 6, effect of variation of well length and distance from tip of well to the lateral boundary of the reservoir were studied. As shown in Figure 6, as well length increases, the rate of decline in pressure increases. Dimensionless pressure increases as well length increases. As dimensionless well length increases, there were ease of crossflow and degree of crossflow. As shown in Figure 5, as distance from tip of well to the lateral boundary of the reservoir increases, the rate of decline in pressure increases. Dimensionless pressure increases as well distance from tip of well to the lateral boundary of the reservoir increases.

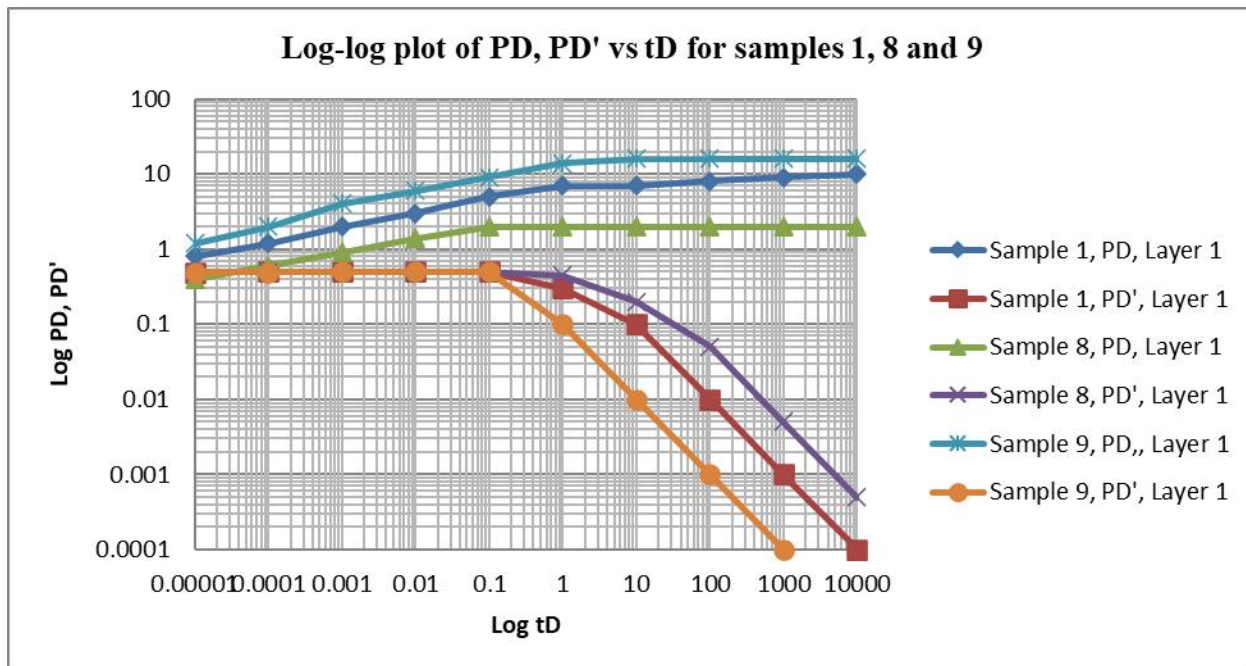


Figure 6: Assessment of response of crossflow due to effect variation of dimensionless well length, L_D and dimensionless distance from tip of well to the lateral boundary of the reservoir, D_{xD} .

3.2.4. Effect of dimensionless reservoir length, x_{eD} , dimensionless distance of centre of well from the lateral boundary of the reservoir, x_{wD} and dimensionless distance from tip of well to the lateral boundary of the reservoir, D_{xD} on crossflow

Cases 10 and 11 were variations of dimensionless reservoir length, x_{eD} ; dimensionless distance of centre of the well from the lateral boundary of the reservoir, x_{wD} ; and dimensionless distance from the tip of the well to the lateral boundary of the reservoir, D_{xD} . Thus, as shown in Figure 7, the effect of variation in reservoir length, the distance of the center of the well from the lateral boundary of the reservoir, and the distance from the tip of the well to the lateral boundary of the reservoir were studied. As shown in Figure 4, as reservoir length increases, the rate of decline in pressure increases. Dimensionless pressure increases as reservoir length increases. As shown in Figure 7, as the distance of the center of the well from the lateral boundary of the reservoir increases, the rate of decline in pressure increases. Dimensionless pressure increases as the distance of the centre of the well from the lateral boundary of the reservoir increases.

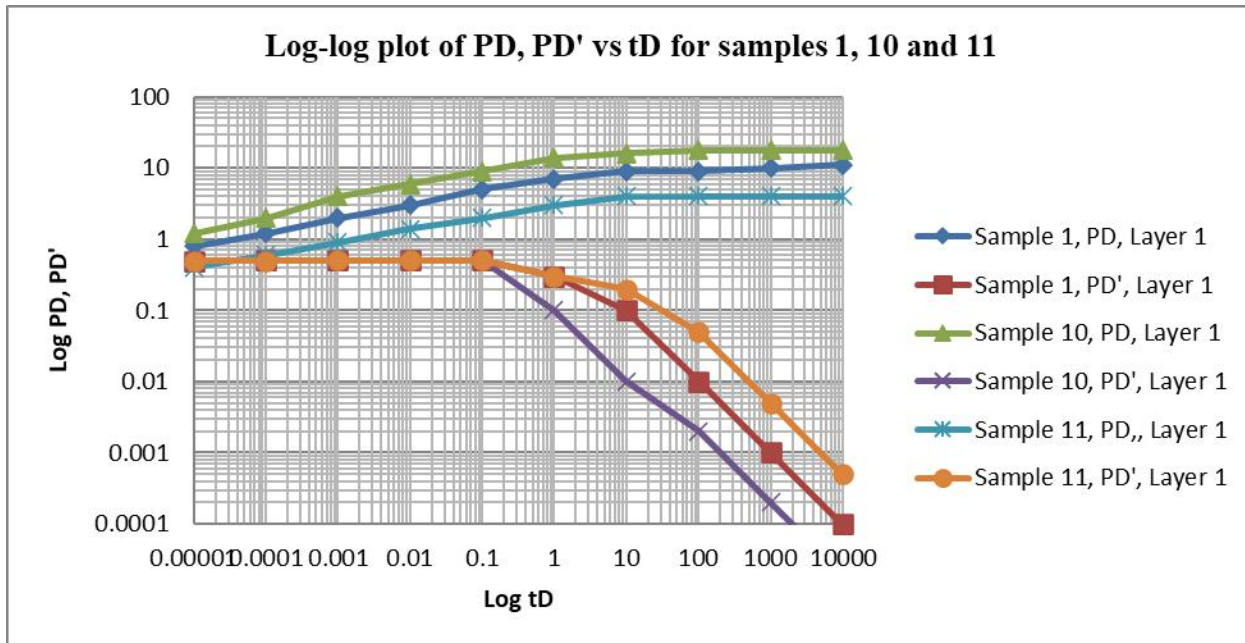


Figure 7: Assessment of response of crossflow due to effect dimensionless reservoir length, x_{eD} , dimensionless distance of centre of well from the lateral boundary of the reservoir, x_{wD} and dimensionless distance from tip of well to the lateral boundary of the reservoir, D_{xD} .

3.2.5. Effect of dimensionless reservoir width, y_{eD} and dimensionless distance from centre of well to the boundary of the reservoir, y_{wD} on crossflow

Cases 12 and 13 were variations of dimensionless reservoir width, y_{eD} , and dimensionless distance from centre of the well to the boundary of the reservoir, y_{wD} . Thus, the effect of variation of reservoir width and distance from centre of the well to the boundary of the reservoir were studied and are shown in Figure 8. As shown in the figure, as the reservoir width increases, the rate of decline in pressure increases. Dimensionless pressure increases as reservoir width increases. As dimensionless reservoir width increases, it leads to ease of crossflow and degree of crossflow.

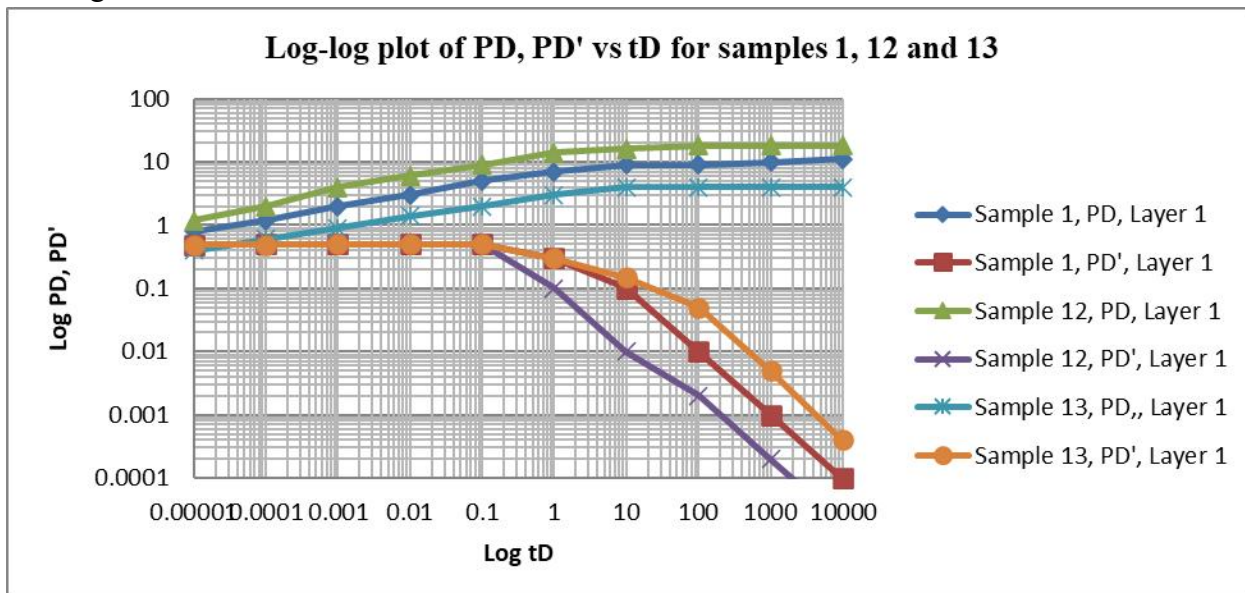


Figure 8: Assessment of response of crossflow due to effect variation of dimensionless reservoir width, y_{eD} and dimensionless distance from centre of well to the boundary of the reservoir, y_{wD} .

Also shown in Figure 8, as the distance from centre of the well to the boundary of the reservoir increases, the rate of decline in pressure increases. Dimensionless pressure increases as the distance from centre of the well to the boundary of the reservoir increases. As dimensionless distance from centre of the well to the boundary of the reservoir increases, similarly for ease of crossflow and degree of crossflow.

3.2.6. Effect of variation of time normalization factor, α on crossflow

Cases 14 and 15 were variations of the time normalization factor. Thus, as shown in Figure 9, the effect of variation of the time normalization factor was studied. As shown in Figure 8, as the time normalization factor increases. As the time normalization factor increases, Ease of crossflow, Degree of crossflow. When the time normalization factor is less than one, Ease of crossflow, Degree of crossflow. But the time normalization factor is less than one. Ease of crossflow, Degree of crossflow

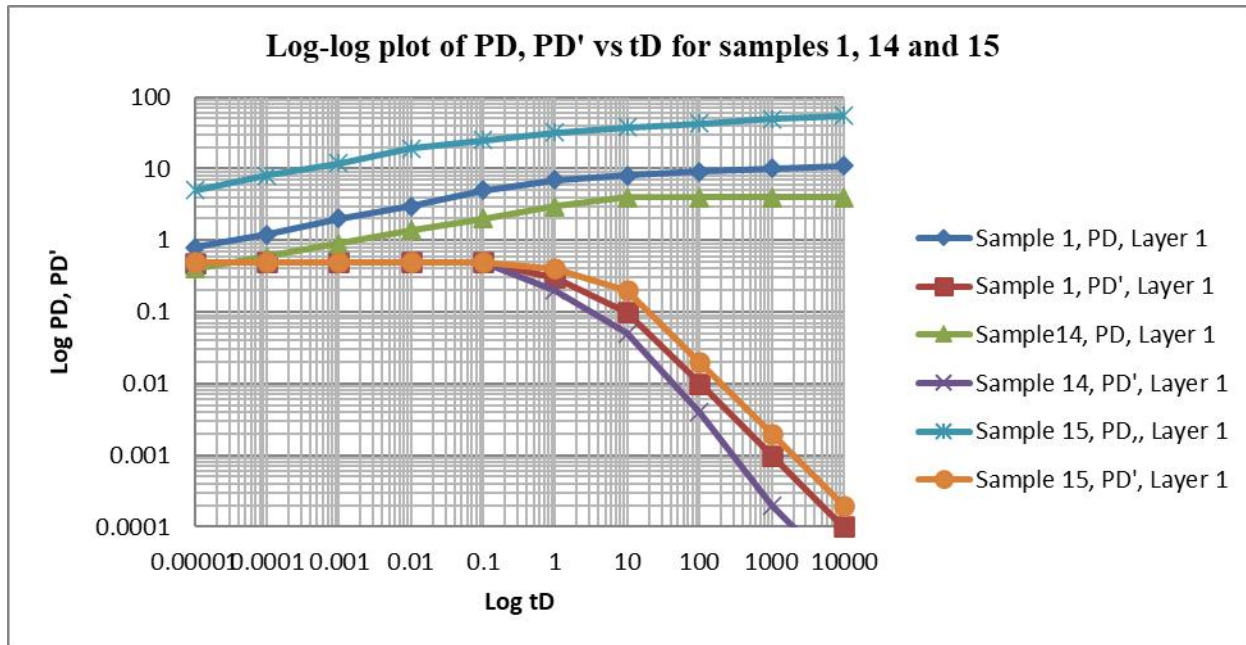


Figure 9: Assessment of response of crossflow due to effect of variation of time normalization factor, α .

3.2.7. Effect of variation of mobility ratio, M , on crossflow

Cases 16 and 17 were variations of the mobility ratio, M . Thus, as shown in Figure 10, the effect of variation of the mobility ratio was studied. As shown in Figure 10, as the mobility ratio increases. As the time mobility ratio increases, there is ease of crossflow and the degree of crossflow. Similarly, the phenomenon was observed when the mobility ratio was less than one.

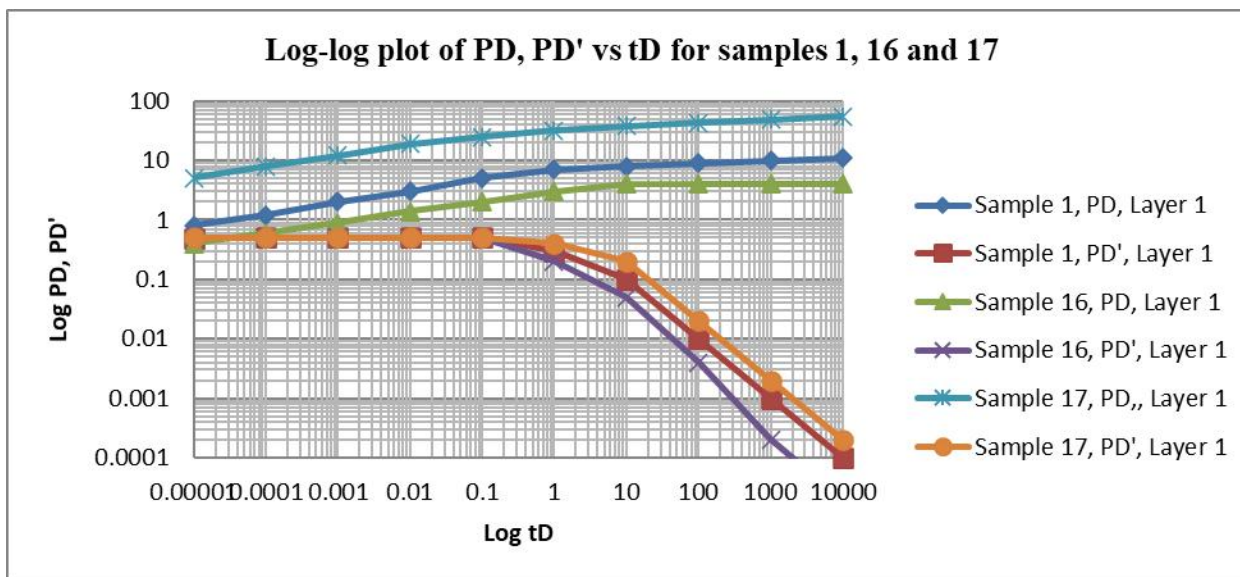


Figure 10: Assessment of response of crossflow due to effect of variation of mobility ratio, M .

It is a common practice to model layered reservoirs as a single compartment by averaging the reservoir parameters associated with each reservoir layer. However, this practice is inadequate as the pressure of each layer changes independently. Changes in pressure from each layer affect the entire performance of the reservoir; they may lead to inter-layer flow, fluid bypass, or premature depletion of a particular layer. Understanding reservoir performance requires knowledge of the permeability and skin factor of each layer (Shahrian *et al.* 2021). When considering the effect of layering, properties of each layer should be different. Factors such as α and M were used. For the crossflow interface, factors A and B were incorporated.

For the set of data considered, the flow regime that subsisted and their intervals depend on the reservoir system parameters. It was also observed that some flow regimes cannot coexist. In some instances, where two consecutive flow regimes overlap, i.e., another flow regime starts when the other has not fully died down, only the fully established one was shown since the other was masked. When the value of factors was not unity, the effect of layering was observed. In such a case, otherwise, it means there is no layering. As soon as there is crossflow, the pressure declines and tends to zero. Hence, the subsequent flow regime is masked.

All boundaries felt this was a complete linear flow regime. The dimensionless pressure and its rapid rise indicate a completely sealed reservoir. The pressure decline is proportional to the rate of depletion. It signals the end of the economic life of the well. Results show that when the layer factors are zero, the reservoir behaves as a single-compartment reservoir. Pressure response was observed to increase steadily. But for other values, the effect of layering is exhibited.

3.4 Identification of Layered and Single Compartment Reservoir

When the value of factors is not unity, the effect of layering was observed. In such a case, . Otherwise, when it means there is no layering. Such a reservoir is a single compartment. As soon as there is crossflow, the dimensionless pressure derivative starts to decline and tends to zero, while dimensionless pressure straightens horizontally. During crossflow from the other layer, there is maintenance of pressure in the producing layer. Hence, the subsequent flow regime is masked. It is necessary to note that there may be layering without crossflow. For layering with crossflow, the condition that must be met is that. The rule is that M can only exist given, but the reverse is an exception.

Conclusion

The mathematical model presented uses the correlation for delineating flow regimes. Therefore, the number of flow regimes, type of flow regime, and interval of subsistence are determined by the reservoir system parameters. Other features of this model are

A far-reaching pressure distribution model of a two-layered bounded reservoir has been developed. In a flow period, it is not possible to have all the possible flow regimes; some will not exist depending on the reservoir system parameters, architecture of the reservoir system, and the fluid properties. Also, preceding flow regimes also determine the type that may follow. Therefore, unlike in most models in which the author decides the flow regime that occurs, the flow regime that may occur and the duration of existence are determined by the values of parameters, geometry of the reservoir, fluid properties, and well architecture selected.

The model was seen to produce a series of radial and linear flows along the individual principal axes or combinations of any of the three principal axes. Each flow regime could be recognized by its characteristic signature in the log-log graph plots of the pressure and pressure derivative versus time.

Although initially the permeability along the principal axes was determined ($k_x > k_z > k_y$) for easy understanding, the imposition of assumption was relaxed during derivation of the model. The order can change depending on the choice of parameters along any of the axes. Similarly, the imposition of layering on the reservoir can be relaxed to a single-compartment reservoir by choosing parameters in the layers to be the same. Such is the flexibility of the model in this article.

Correlation for delineating the interval of the flow regime in a single-compartment reservoir has been extended to layered reservoirs. The interval of existence depends on the reservoir system parameters. The existence of some flow regimes obliterates other flow regimes. Also, when the interval of subsistence is short, the flow regime is masked and not observed.

References

- Bourdet D. (1985). "Pressure behaviour of layered reservoir with crossflow". *Society of Petroleum Engineers*, SPE Paper No. 13628, presented at the 1985 Annual California Regional Meeting in Bakers, CA., Mar. 27 – 29.
- Russel D. G. and Prats M. (1962). "Practical aspects of interlayer crossflow". *Journal of Petroleum Technology*. Pp 589 - 594. Reprint Series No. 9- "Pressure Analysis Methods", *Society of Petroleum Engineers* of AIME, Dallas (1967). Pg. 120 -125.
- Du K-F. and Stewart G. (1992). "Transient pressure response of horizontal well in layered and naturally fractured reservoirs with Dual-porosity behaviour. *Society of Petroleum Engineers*, SPE 24682. Pg. 227 – 240.
- Owolabi A. F., Olafuyi O. A., Adewole E. S. (2012). "Pressure distribution in a layered reservoir with gas cap and bottom water". *Nigerian Journal of Technology (NIJOTECH)*, Vol. 31, No. 2, July. Pg. 189 – 198.
- Adewole E. S., Rai B. M. and Audu T. O. K. (2003). "Pressure distribution in a layered reservoir with lateral wells. *Journal for Nigerian Association of Mathematical Physics*. Vol. 7. Pg. 135 – 146.\
- Kuchuk, F.J and Habashy T. (1996). 'Pressure behavior of Horizontal Wells in Multilayer Reservoirs with Crossflow' SPE formation Evaluation, March. Pg 55-64

Lu J., Rahman M. M., Yang E., Alhamami M. T., Zhong H (2021). “Pressure transient behavior in a multilayer reservoir with formation crossflow”. *Journal of Petroleum Science and Engineering*. Volume 208, Part B, January <https://doi.org/10.1016/j.petrol.2021.109376>.

Ehlig-Economides, C.A., and Joseph, J.A. (1995). “A New Test for Determination of Individual Layer Properties in a Multilayered Reservoir”. *Society of Petroleum Engineers*, SPE Paper No. 14167, Presented at 1985 SPE Annual Technical Conference and Exhibition, Las Vegas, NV., Sept. 22-25.

Oloro J., Adewole E.S. And Olafuyi O.A., (2012). “Pressure Distribution of Horizontal Wells in a Layered Reservoir with Simultaneous Gas Cap and Bottom Water Drives”. *American Journal of Engineering Research (AJER)*. Vol. 3, Issue – 12. Pg 41-53

Viana I., Bela R. V., Pesco S., Barreto A. Junior, (2022). “An analytical model for pressure behavior in multilayered radially composite reservoir with formation crossflow”. *Journal of Petroleum Exploration and Production Technology*. <https://doi.org/10.1007/s13202-022-01460-x>

Wang J., Wang X., Dong W.. “Rate decline curves analysis of multiple-fractured horizontal wells in heterogeneous reservoirs”. *Journal of Hydrology*. Volume 553, October 2017, Pages 527-539. <https://doi.org/10.1016/j.jhydrol.2017.08.024>

Odeh A. S. and Babu D.K. (1990), “Transient Flow Behavior of Horizontal Wells: Pressure Drawdown and Buildup Analysis” *SPE Formation Evaluation*, March, Pg 10-14.

Al-Rbeawi S. and Tiab D. (2013), “Transient Pressure of Horizontal Wells in a Multi-Boundary System” *American Journal of Engineering Research (AJER)*, Volume 2, Issue 4. Pg 44-66.

Chu H., Liao X., Chen Z., Zhao X., Liu W., Dong P. (2019). “Transient pressure analysis of a horizontal well with multiple, arbitrarily shaped horizontal fractures”. *Journal of Petroleum Science and Engineering journal*. <https://doi.org/10.1016/j.petrol.2019.06.003>

Gringarten A.C., and Ramey H.J. Jr, (1973). “The use of Source and Green’s Functions in solving Unsteady-flow Problems in Reservoirs”. *Society of Petroleum Engineers Journal*. Vol. 13, Pg.285-296.

Shahrian E., and Masihi M. (2021) Analysis of well testing results for single phase flow in reservoirs with percolation structure. *Oil & Gas Science and Technology – Rev. IFP Energies nouvelles* 76, 15 (2021). <https://doi.org/10.2516/ogst/2020092>.

Ogbue, M. C. and Adewole, E. S. (2013). ‘Theoretical Investigation of Factors Affecting Water Breakthrough Time in a Horizontal Well Subject to Bottom Water Drive’. *Trans Tech Publications Inc. Material Science & Engineering*, Switzerland, vol. 824, page 394-400.

Nomenclature

$$r_{weq} = \left[\left(\frac{k}{k_z} \right)^{0.25} + \left(\frac{k_z}{k} \right)^{0.25} \right] \dots\dots\dots 9$$

$$r_{wD} = \frac{2r_{weq}}{2} \dots\dots\dots 10$$

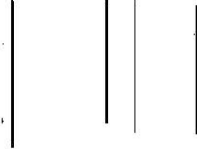
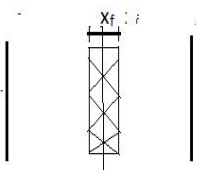
$$P_D = \frac{kh\Delta P}{141.2q\mu B_0} \dots\dots\dots 11$$

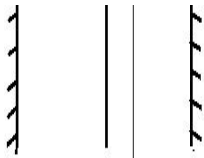
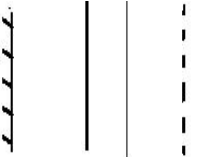
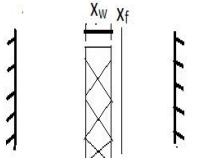
$$t_D = \frac{0.001056kt}{\phi\mu C_t L^2} \dots\dots\dots 12$$

$k = \sqrt[3]{k_x k_y k_z}$	13
$L_D = \frac{L}{2h} \sqrt{\frac{k}{k_x}}$	14
$x_D = \frac{2x}{L} \sqrt{\frac{k}{k_x}}$	15
$x_{eD} = \frac{2x_e}{L} \sqrt{\frac{k}{k_x}}$	16
$x_{wD} = \frac{2x_w}{L} \sqrt{\frac{k}{k_x}}$	17
$y_D = \frac{2y}{L} \sqrt{\frac{k}{k_y}}$	18
$y_{eD} = \frac{2y_e}{L} \sqrt{\frac{k}{k_y}}$	19
$y_{wD} = \frac{2y_w}{L} \sqrt{\frac{k}{k_y}}$	20
$z_D = \frac{2z}{L} \sqrt{\frac{k}{k_z}}$	21
$z_{eD} = \frac{2z_e}{L} \sqrt{\frac{k}{k_z}}$	22
$z_{wD} = \frac{2z_w}{L} \sqrt{\frac{k}{k_z}}$	23
$d_x = D_x = \frac{x_e - L}{2}$	24

Appendix 1

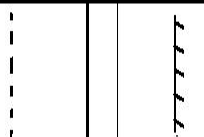
Basic instantaneous source functions (Courtesy of Gringarten A.C. and Ramey H.J.Jr.,
Society of Petroleum Engineers Journal, vol. 13 ,page 289-290, 1973)

$X=0$	X_w	X_e	SOURCE	FUNCTION NUMBER	SOURCE FUNCTION
			INFINITE PLANE SOURCE	I(X)	$\frac{\exp\left[-\frac{(x-x_w)^2}{4n_x t}\right]}{\sqrt[2]{n_x t}}$
			INFINITE SLAB SOURCE	II(X)	$\frac{1}{2} \left[\operatorname{erf} \frac{\frac{x_f}{2} + (x-x_w)}{\sqrt[2]{n_x t}} + \operatorname{erf} \frac{\frac{x_f}{2} - (x-x_w)}{\sqrt[2]{n_x t}} \right]$

	PRESCRIBED FLUX, PLANE SOURCE	VII(X)	$\frac{1}{x_e} \left[1 + 2 \sum_{n=1}^{\infty} \exp\left(-\frac{n^2 \pi^2 n_x t}{x_e^2}\right) \cos \frac{n \pi x_w}{x_e} \cos \frac{n \pi x}{x_e} \right]$
	MIXED BOUNDARY, PLANE SOURCE	IX(X)	$\frac{2}{x_e} \sum_{n=1}^{\infty} \exp\left(-\frac{(2n+1)^2 \pi^2 n_x t}{4 x_e^2}\right) \cos \frac{(2n+1) \pi x_w}{x_e} \cos \frac{(2n+1) \pi x}{x_e}$
	PRESCRIBED FLUX, SLAB SOURCE	X(X)	$\frac{x_f}{x_e} \left[1 + \frac{4 x_e}{\pi x_f} \sum_{n=1}^{\infty} \frac{1}{n} \exp\left(-\frac{n^2 \pi^2 n_x t}{x_e^2}\right) \sin \frac{n \pi x_f}{2 x_e} \cos \frac{n \pi x_w}{x_e} \cos \frac{n \pi x}{x_e} \right]$

Appendix 2.

Extension of Source and Greens Function Table. For the case prescribed pressure at $x=0$ and prescribed flux at $x=L$. This is a lateral inversion of ix (z). Modified form of ix (x), is given as ix (x)'

$x=0$	x_w	x_e	SOURCE	FUNCTION NUMBER	SOURCE FUNCTION
			MIXED BOUNDARY, PLANE SOURCE	IX(X)'	$\frac{2}{x_e} \sum_{n=1}^{\infty} \exp\left(-\frac{(2n-1)^2 \pi^2 n_x t}{4 x_e^2}\right) \sin \frac{(2n-1) \pi x_w}{x_e} \sin \frac{(2n-1) \pi x}{x_e}$